International Journal of Mechatronics and Applied Mechanics
2025, Issue 19, Vol. 1

OPEN ACCESS

HUMAN MACHINE INTERFACE DESIGN OF AR-HUD AUTONOMOUS VEHICLE BASED ON SCENARIO MODEL

Lili Zhou[1]
[1]*Smart Manufacturing College,*
Zhengzhou University of Economics and Business, Zhengzhou, 451191, China

Abstract - A well-designed human-machine interface (HMI) facilitates seamless interaction between drivers and vehicles, particularly when activating autonomous driving functions. This study aims to enhance the HMI of autonomous vehicles by optimizing information interaction during driving, using a situational awareness model. To achieve this, the sparrow search algorithm and simulated annealing algorithm were employed to evaluate and improve the display of head-up display (HUD) interface icons. The results revealed a strong positive correlation between the A1 and A2 modules, as well as between the A5 and A6 modules, indicating that drivers tend to focus on highly correlated modules when engaging with specific elements of the interface. By integrating simulated annealing into the sparrow search algorithm, the study achieved the model's optimal solution. Notably, the accuracy of speech recognition technology improved from 85.12% to 95.32%, and gesture recognition accuracy increased from 80.24% to 90.67%. Additionally, the response times of the HMI and touch technology decreased from 0.581s to 0.462s and from 0.302s to 0.212s, respectively. These improvements highlight significant gains in both response speed and accuracy. The augmented reality HUD, developed based on the situational awareness model, effectively enhances user interaction and safety in autonomous vehicles. This study offers a valuable framework for designing and evaluating future HMI systems in autonomous driving contexts.

Keywords: Situational awareness model, AR-HUD, Human-computer interface design, Visual area. SA-SSA algorithm

1. Introduction

The evolution of autonomous driving technology has transformed vehicles from mere modes of transportation into mobile spaces that integrate various intelligent systems [1-2]. In this shift, Human-Computer Interface (HCI) design plays a crucial role in enhancing both user experience and driving safety. Augmented Reality Head-Up Displays (AR-HUD), as a cutting-edge HCI technology, offer drivers a more intuitive and efficient way to interact with information by projecting virtual data onto the real-world environment [3-4]. Since drivers have varying information needs and processing capacities, creating adaptable and personalized HCI systems has become a significant research focus.

Several scholars have explored automotive HCI design. Jiang et al. proposed a multi-degree display adjustment system using near-field and far-field images to improve driver attention and vehicle synchronization, optimizing the interactive interface. This system-maintained image quality even when the optical path shifted by 25mm, enhancing multi-depth display [5]. Fan et al. introduced an off-axis reflective optical structure based on a dual focal plane display for an ideal AR-HUD. This system required multiple focal planes to enable basic driver interaction and included an automated analysis program to evaluate modulation transmission functions and distortion. The maximum distortion of far-field and near-field images was 3.15% and 3.58%, respectively, meeting interaction and display expansion needs [6]. Goodge et al. suggested optimizing the display interface based on gaze tracking to improve the evaluation of driving performance indicators. This method enhanced HCI interaction and contributed to safer driving and a better user experience [7]. Bing et al. developed a real-time system for publishing HCI data based on AI-driven behavior recognition, offering vehicle position detection, collision warnings, and fatigue monitoring. This system improved the HCI experience and alleviated drivers' psychological burden [8].

https://doi.org/10.17683/ijomam/issue19

The main goal of the research is to propose a new human-machine interface design scheme by optimizing the situational awareness model and combining with AR-HUD technology. At the same time, Sparrow Search Algorithm (SSA) combined with Simulated Annealing algorithm (SA) is introduced to optimize the interface icon and layout. This study provides a reference for the development direction of future intelligent transportation systems, aiming to improve the efficiency of information transmission and driving safety by optimizing HCI design, while reducing the cognitive load on drivers.

2. Methods and Materials

2.1Construction based on SA Model

When studying the HCI design of autonomous vehicle, it is needed to first understand the SA model in depth. As a key theoretical framework for understanding how individuals perceive, understand, and predict changes in their surrounding environment, SA model plays a crucial role in HCI design in autonomous vehicle [9-10]. The study improved the situational awareness model by making decision-making information and action sequence information independent of each other and situational awareness, and situational awareness as a prerequisite for drivers to clarify decision-making information and take actions. The improved model takes into account the influence of drivers' driving experience, memory ability, and information processing ability on situational awareness. The SA model can be mainly divided into three levels, namely perception of elements in the environment, understanding of the current situation, and prediction of future states. At the perceptual level, drivers mainly collect situational information about actual road conditions based on their auditory and visual systems, including the current driving status of vehicles and road congestion. At the level of understanding, drivers make corresponding judgments and interpretations of the perceived information, and take certain measures when appropriate, such as reducing speed in advance to avoid collisions if there are pedestrians on the sidewalk ahead. At the prediction level, based on the information of perception and understanding levels, necessary measures have been taken for the current road condition information, such as the signal light ahead turning red and the driver being unable to drive through the intersection at the current speed. Therefore, the driver takes slow measures to slow down to the intersection [11-12]. Improvements have been made based on the three-level SA model by combining road condition information and interaction processes. The improved SA model structure is shown in Fig.1.

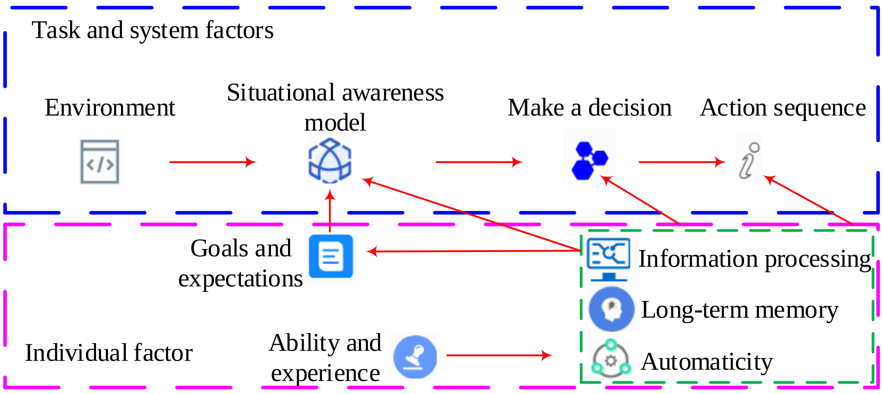

Figure 1: The structure diagram of the optimized SA model

In Fig.1, the SA model has been improved to ensure that decision information and action sequence information are independent of SA. SA, as a prerequisite for drivers to clarify decision-making information and take corresponding measures, is also influenced by the driver's driving experience, memory ability, information processing ability, and goals. In the SA model, there is a certain functional correspondence between SA level and time, which is mathematically expressed as formula (1).

$$S(t_1,t_2)=A\frac{E_{MAX}}{E_R}(1-e^{-B\frac{E_{\max}}{E_R}(t_1-t_2)}) \tag{1}$$

In formula (1), A and B are fitting parameters. $E_{\max}$ is the driver's maximum visual range. E_R is the level of effort required for drivers to achieve standard awareness. S is the functional relationship. The factors that affect the driver's SA driving can mainly be divided into the driver's own factors, namely the driver's personal psychological and physiological conditions, as well as the interaction between the car and the driving environment. This includes road congestion and traffic flow. The representation of emotional awareness mainly depends on the degree to which the driver completes the driving task. The current methods used for SA mainly include physiological indicators, user recall and description, performance, and SA scales. Physiological indicators mainly include EEG signals, eye movements, and other physiological indicators to determine the driver's SA. User recall and description mainly rely on the user's review and description of relevant information after the task is completed. Performance is evaluated by observing users' completion of tasks to assess SA level. The SA scale is mainly used by users to conduct self-evaluation based on their SA level. The SA model is integrated into AR-HUD to optimize HCI design. The HCI design of AR-HUD based on SA level indicator is shown in Fig.2.

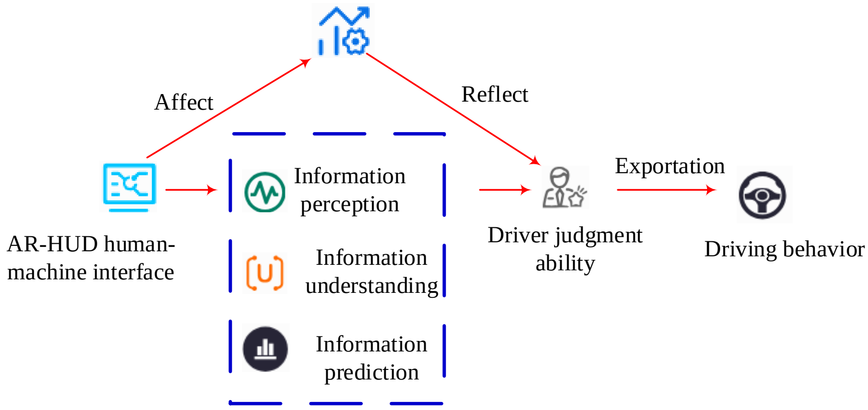

Figure 2: HCI design of AR-HUD based on SA level index

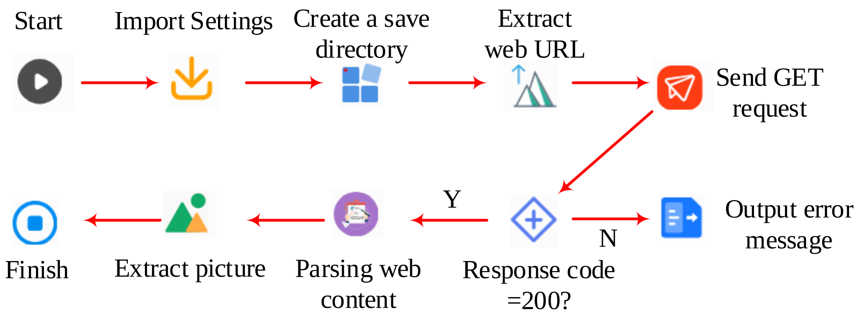

Figure 3: Crawler-based flowchart

2.2 HCI Evaluation and Optimization Method for AR-HUD System

Before designing the interactive interface, it is often necessary to build a set of icon samples for the AR-HUD interface. This study constructs a crawler program based on Python technology to obtain image information. The crawler extracts icon samples related to driving scenarios from web resources based on keyword search and image recognition techniques. In addition, icon extraction is optimized by combining deep interviews to ensure the quality and applicability of the sample set. The program flow based on crawlers is shown in Fig.3.

After constructing the icon sample set based on the crawler program, the modules are decomposed based on the unique functions of individual icons, and icons with similar functions are grouped together to complete the construction of the interface element sample set. To better select the icon sample set, this study optimizes the extraction of icons through in-depth interviews. Firstly, relevant keywords are extracted, and an icon evaluation index acquisition system based on AR-HUD interface is constructed from three dimensions: interview preparation, interview execution, and interview completion. Interview preparation aims to prepare in advance for the information that may be obtained during the interview, to ensure the smooth progress of the interview process. The interview execution aims to facilitate effective and easy communication with the interviewer. After the interview, the content of the interview is organized and keywords are extracted. This study introduces the entropy weight method to screen the indicators obtained from interviews for icons. By standardizing the icon samples and then calculating the weight value of each index based on information entropy. The comprehensive scores of all icons are evaluated by linear weighting method, so as to filter out the icons with higher importance. The standardization operation is carried out first. After standardization, individual icons are scored on a percentage scale [13-14]. The relevant expression is shown in formula (2).

$$X_{\tilde{ab}} = \frac{X_{ab} - \min(X_a)}{\max(X_a) - \min(X_a)} \tag{2}$$

In formula (2), $X_{ab}^{\sim}$ is the standardized percentage score. X_{ab} is the percentage score for the b-th indicator of the first a icon. max and min are the maximum and minimum values respectively. Based on a standardized percentage scoring system, the proportion of a single indicator under the corresponding icon can be calculated, as shown in formula (3).

$$P_{ab} = \frac{X_{ab}}{\sum_{a=1}^{n} X_{ab}} \tag{3}$$

In formula (3), P_{ab} is the proportion of a single icon. Based on the definition of information entropy, the calculation of information entropy for all indicators is shown in formula (4).

$$E_b = -In(m)^{-1}\sum_{a=1}^{m} P_{ab} InP_{ab} \tag{4}$$

In formula (4), E_b is the information entropy. After obtaining the information entropy of each indicator based on formula (4), the expression of the weight values of each indicator is further calculated as shown in formula (5).

$$w_b = \frac{1-E_b}{k-\sum E_b} \tag{5}$$

In formula (5), k is the number of icons. Finally, based on the weight values of individual indicators, the comprehensive score of all icons is evaluated using linear weighting method, as shown in formula (6).

$$SC_a = \sum_{b=1}^{n} w_b \bullet P_{ab} \tag{6}$$

In formula (6), SC_a is the comprehensive score of the icon. In the interface of AR-HUD, drivers may have different levels of attention to different icons based on different road conditions. Therefore, this study first optimizes the interface layout model based on icon importance. After sorting all icons according to their importance, the gray weighting method is used to represent the frequency of individual icon usage, and then the importance of the icons is obtained by combining their importance and frequency [15-16]. Based on the icon module set and the attribute set of the module, the mathematical calculation of the ordinal number is shown in formula (7).

$$c_{ab} = \begin{Bmatrix} 1 & T_a \succ T_b \\ 0.5 & T_a = T_b \\ 0 & T_a \prec T_b \end{Bmatrix} \tag{7}$$

In formula (7), T is the attribute set composed of modules. After defining the icon viewing frequency rating matrix, and combining the importance level, relevance of icon elements, and frequency for summation, the mathematical expression of the importance of a single icon is shown in formula (8).

$$\begin{cases} \mu_a = \omega_1 I_a + \omega_2 R_a \\ I_a = \sum_{b\in N} c_{ab} \\ R_a = K_a \bullet J_a \end{cases} \tag{8}$$

In formula (8), μ_a represents the importance of the icon module. ω_1 is the weight value of the icon module. ω_2 is the weight of viewing frequency. I_a is the importance of the icon module. R_a is the viewing frequency of the icon. K_a is the viewing frequency rating of the icon. J_a is the probability of module occurrence. Subsequently, optimization is carried out for different visual levels of the icon module, combining the driver's scanning range with the interactive interface to obtain the approximate field of view of the AR-HUD interface, as shown in Fig.4.

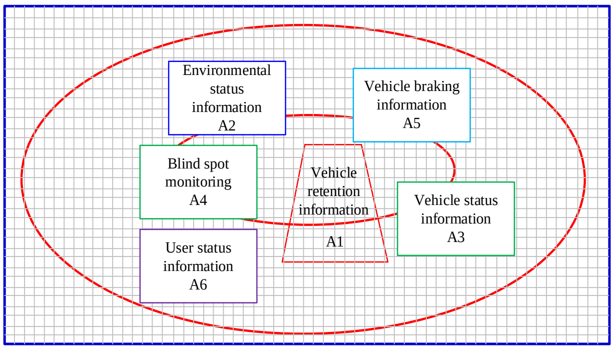

Figure 4: Field of view distribution diagram of AR-HUD module interface

In Fig. 4, the information modules within the field of view are decomposed into six regions, and the area of the modules can be calculated based on the basic unit area. The expression based on visual allocation is shown in formula (9).

$$\begin{cases} D_a = \sum_{a=1}^{m} \gamma_{ak} \cdot S_a \cdot \mu_a \\ S_a = lu_i \end{cases} \tag{9}$$

In formula (9), l is the edge length of the basic cell. u_i is the importance of the icon module. m is the total number of icon modules. γ_{ak} is the level of the module in different regions. S_a is the area of the icon module. In the design of AR-HUD, a clean interface is the key to user choice. This study aims to improve the cleanliness and simplicity of the interface by aligning icon modules. The calculation based on the simplicity of the AR-HUD interface is shown in formula (10).

$$g_s = \frac{o_x + o_y}{2o} \tag{10}$$

In formula (10), g_s is the simplicity of the AR-HUD interface. o_x and o_y are the number of modules corresponding to the horizontal and vertical axes. Finally, an objective function is introduced to allocate attention values for interface icons, and the equation based on the objective function is shown in formula (11).

$$f(a) = \max\left[\sum_{a=1}^{m} \lambda_1 D_a + \lambda_2 h_a + \lambda_3 g_s\right] \tag{11}$$

In formula (11), h_a is the distance between icons, and λ_1, λ_2, and λ_3 are the weight values of each indicator. This study introduces SSA to evaluate and optimize HCI design. The core idea is to simulate the interaction between discoverers and followers during the foraging process of sparrows, as well as the reaction mechanism of sparrows when facing danger. In the algorithm, the sparrow population is divided into two roles: discoverer and follower. By simulating real hunting scenarios, the sparrow's danger warning mechanism is added [17-18]. Firstly, the population is initialized by defining the search space as R dimensions and the population size as m. The mathematical expression based on this population is shown in formula (12).

$$Y_a = [y_{a1}, y_{a2}, \cdots y_{aR}], a = 1, 2, \cdots m \tag{12}$$

In formula (12), y_{ab} is the b-th dimensional position where the first a sparrows are located. After obtaining the position of sparrows in the population, the fitness value of sparrows is shown in formula (13).

$$F_a = f(Y_a), a = 1, 2, 3, \cdots m \tag{13}$$

After the initialization of the population is completed, the first step is to update the position of the discoverer, as shown in formula (14).

$$Y_{a,b}^{t+1} = \begin{cases} Y_{a,b}^{t} \cdot \exp\left(\dfrac{-a}{\tau \cdot Iter_{\max}}\right) & if \quad War \prec ST \\ Y_{a,b}^{t} + Q \cdot T & if \quad War \geq ST \end{cases} \tag{14}$$

In formula (14), t is the number of iterations. $Iter_{\max}$ is the maximum number of iterations. τ is a random number between 0-1. War is the warning value. ST is a security parameter. Q is a random number that follows a normal distribution. T is the matrix of $1 \times r$. Secondly, the position of the joiners has been updated, as shown in formula (15).

$$Y_{a,b}^{t+1} = \begin{cases} Y_{a,b}^{t} \cdot \exp\left(\dfrac{y_{worst}^{t} - y_{a,b}^{t}}{a^2}\right) & if \quad a \prec \dfrac{m}{2} \\ Y_P^{t+1} + |Y_{a,b}^{t} - Y_P^{t+1}| \cdot A^{+} \cdot T & Otherwise \end{cases} \tag{15}$$

In formula (15), Y_p is the optimal position of the discoverer at the current stage. Y_{worst} is the worst position in the entire space. Finally, the location of the warning agent is updated, and the result is shown in formula (16).

$$Y_{a,b}^{t+1} = \begin{cases} Y_{best}^{t} + \beta \cdot |Y_{a,b}^{t} - Y_{best}^{t}| & if \quad f_a \succ f_g \\ Y_P^{t+1} + k \cdot \left(\dfrac{|Y_{a,b}^{t} - Y_{worst}^{t}|}{(f_a - f_w) - \varsigma}\right) & if \quad f_a = f_g \end{cases} \tag{16}$$

In formula (16), Y_{best} is the global optimal position. β is the step size control parameter. ς is a constant that ensures the denominator is not zero. f_a is the fitness value of a single sparrow. f_g and f_w are currently the best and worst cases. Considering that SSA is prone to getting stuck in local optima, this study introduces Simulated Annealing (SA) algorithm to optimize SSA. Using the global optimization capability of SA and the fast convergence characteristics of SSA to optimize the interface icon layout, avoiding the problem that SSA may fall into the local optimum when used alone. The Metropolis criterion based on SA algorithm is shown in formula (17).

$$p = \begin{cases} 1 & if \quad E(x_{new}) \prec E(x_{old}) \\ \exp\left(-\dfrac{E(x_{new}) - E(x_{old})}{T}\right) & if \quad E(x_{new}) \geq E(x_{old}) \end{cases} \tag{17}$$

In formula (17), T is temperature. x_{new} and x_{old} are the new and current solutions.

2.3 Analysis of HCI Design Based on AR-HUD

After determining the optimization method for the interactive interface, based on the situational information of road conditions, the AR-HUD interface can be combined with SA to divide the AR-HUD system interface into six parts. The first part is the user status information column. After the driver monitoring system performs image recognition on the driver's facial features, it uses real-time intelligent analysis to determine whether the driver is in dangerous situations such as distracted driving or making phone calls. If there is a dangerous situation, the AR-HUD interface is used for real-time alarm. The second part is the vehicle status information section, which reflects information such as vehicle speed, fuel level, and mileage. The third part is vehicle maintenance information, relying on driving assistance systems and collision warning systems, detecting the position relationship between vehicles, pedestrians, and other vehicles through radar information and infrared camera technology, and displaying it through the AR-HUD interface. The fourth part is the vehicle braking information, mainly including deceleration icons and emergency braking.

The fifth part is environmental status information, which provides traffic information to drivers through road traffic signs and is displayed in the AR-HUD interface. The sixth part is an environmental warning system based on blind spot monitoring and panoramic imaging, which alerts drivers to the risks around the vehicle through cameras around the vehicle. After confirming the components of the AR-HUD interface, this study refers to the AR-HUD information interface of several typical car models, as shown in Fig.5.

In Fig. 5, although the AR-HUD interfaces of the four typical vehicle models are presented in different ways, the modules included are basically the same, all of which involve driving information, current speed, path planning, fuel consumption, etc. However, overall there is a lack of display of driver entertainment behaviors, such as current music, video information, etc. Based on the AR-HUD interfaces of various vehicle models, this study ultimately designs an interface layout diagram based on AR-HUD, as shown in Fig.6.

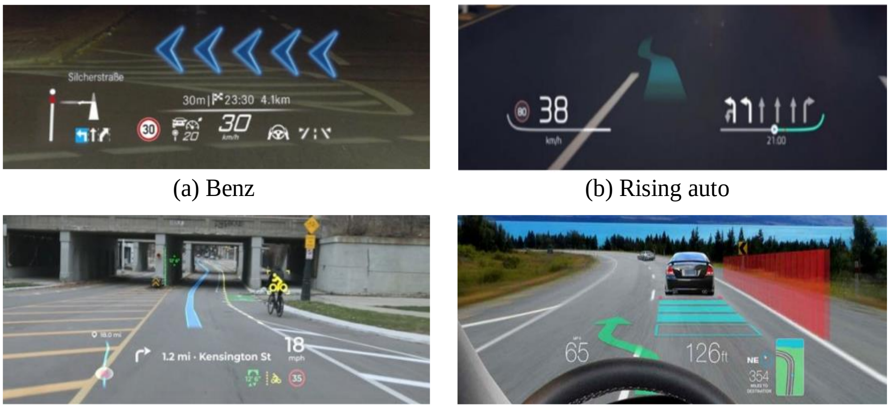

(a) Benz (b) Rising auto

(c) Volkswagen (d) Chery AUTOMOBILE Co., Ltd

Figure 5: AR-HUD interface diagram of a typical vehicle

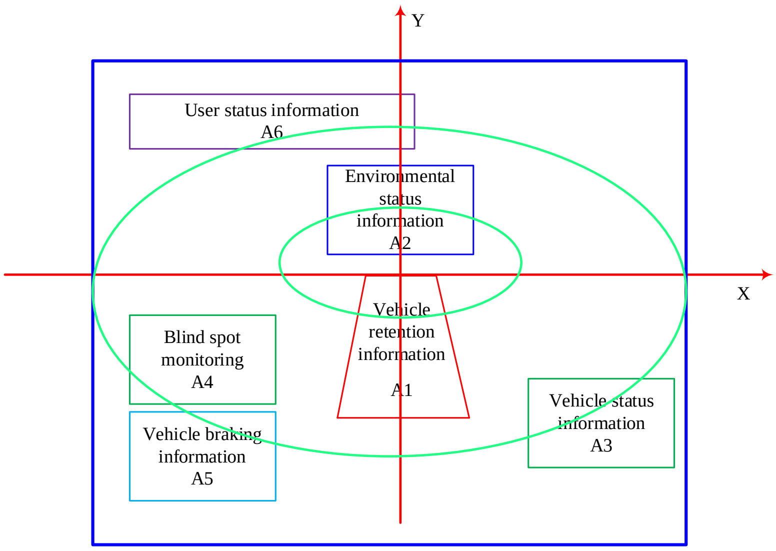

Figure 6: Layout design based on AR-HUD interface information

Figure 6 shows the layout design of the AR-HUD interface information. Among them, A1 is located in the lower center of the interface, which is mainly used to display the current state of the vehicle, such as speed, fuel, mileage and other basic information, which is one of the most frequently viewed information by the driver, and provides immediate feedback on the running status of the vehicle. A2 is located in the center of the interface and is mainly used to display environmental information around the vehicle, such as traffic signs, road conditions, weather, etc., which helps drivers understand the current driving environment and make corresponding driving decisions. Located in the lower right corner of the interface, A3 provides detailed vehicle status information, such as engine status, fault warnings, etc., which is crucial for drivers who need to monitor the health of the vehicle. A4 is located in the lower left corner of the interface and mainly displays whether there are other vehicles or obstacles in the blind zone of the vehicle, which can improve the safety of driving, especially when changing lanes or overtaking. A5 is located in the left center of the interface, which is mainly used to display the braking status of the vehicle, such as emergency braking warning, braking system status, etc., which plays an important role in preventing accidents and improving driving safety. A6, located in the upper left corner of the interface, is mainly used to monitor the driver's state, such as fatigue, concentration, etc. By monitoring the driver's state, the system can provide corresponding warnings or suggestions to improve driving safety. Finally, the specific flow of the research work is shown in Figure 7.

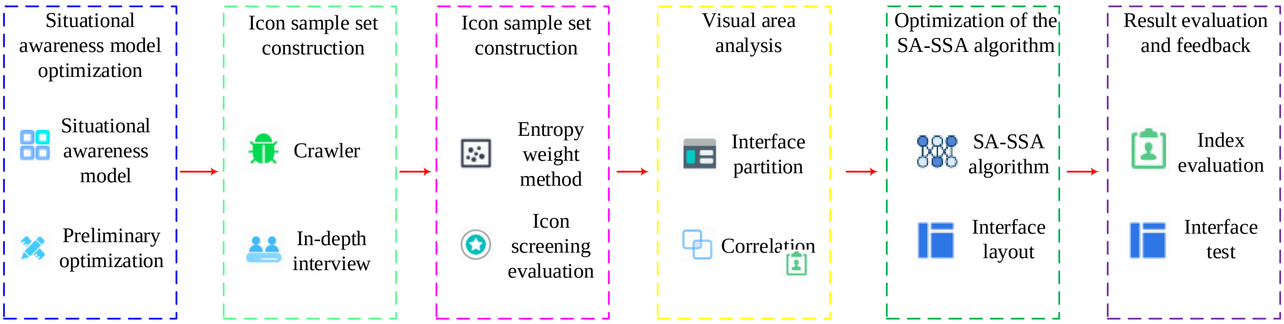

Figure 7: Human Machine Interface Design Process for Autonomous Vehicles

In Fig. 7, the human-computer interface design is initially optimized based on the situational awareness model. Secondly, the icon samples are obtained through the crawler program, and the icon extraction is optimized based on the in-depth interview to complete the construction of the icon sample set; subsequently, the entropy weighting method is used to filter and evaluate the icons to complete the icon evaluation and filtering; immediately after that, based on the division of the visual area of the AR-HUD interface, the correlation between the modules is analyzed to complete the visual area analysis; the interface layout is optimized using the SA-SSA algorithm; finally, the user testing of the optimized interface is conducted to evaluate the effectiveness of the design. Finally, the optimized interface is tested by users to evaluate the effectiveness of the design.

3. Results

3.1 Visual Region Analysis Based on AR-HUD Interface

Based on the AR-HUD interface diagram constructed above, the visual center is defined as the coordinate origin. After constructing a 2D coordinate system, the A1-A6 areas are coordinated. Table 1 shows the size information of each module based on the AR-HUD interface.

Table1. Detailed dimensional information for the module

Module/mm	Length	Width	Area
A1	70/250	250	40000
A2	250	150	37500
A3	250	80	20000
A4	250	80	20000
A5	300	50	15000
A6	550	50	27500

After coordinating the modules based on the information in Table 1, 30 experts are selected to score individual modules on the AR-HUD interface. After constructing the matrix of module importance and viewing frequency, the comprehensive importance of six modules is constructed based on the importance and viewing matrix, as shown in Fig.8.

Figs.8 (a) and (b) compare the importance and viewing frequency of modules A1-A3 and A4-A6. In Fig.8 (a), the values of the basic importance and total importance A2 modules are both at the highest level, with values of 0.220 and 0.213. At the same time, the area with the highest viewing frequency is the A1 area, with a value of 0.225. In Fig.8 (b), the importance and viewing frequency of the A4 area are higher than those of the other areas, with basic importance, viewing frequency, and total importance values of 0.181, 0.164, and 0.171. In summary, the correlation analysis results show that the interface reaction time, touch technology reaction time and sight off road time are significantly reduced after optimization by the SA-SSA algorithm.

This indicates that the optimized interface has a significant improvement in reaction speed as well as accuracy, which can effectively improve the interaction experience and safety of self-driving cars. This study further calculates the correlation coefficients between modules based on the cognitive abilities of drivers during the driving process, as shown in Table 2.

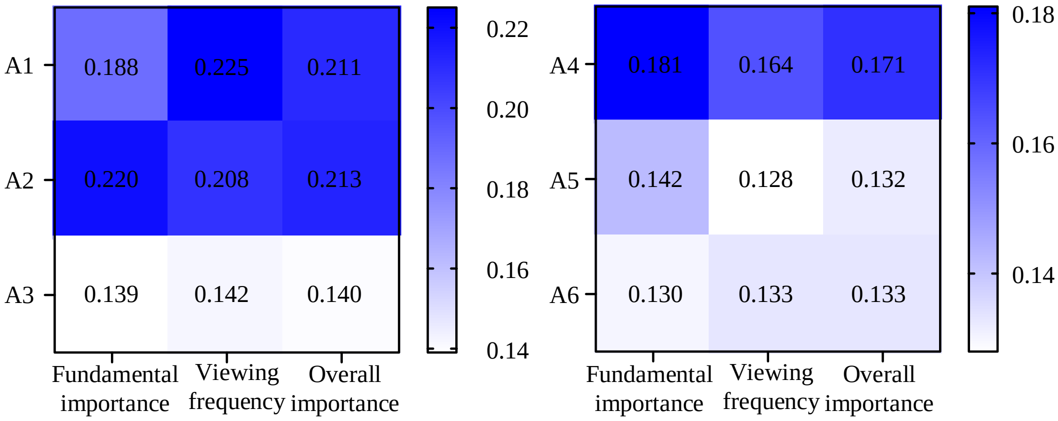

(a) Comparison of A1-A3 importance and viewing frequency

(b) Comparison of A4-A6 importance and viewing frequency

Figure 8: Icon module importance index and viewing frequency comparison

Table 2. Correlation coefficient between modules

Chart information module	A1	A2	A3	A4	A5	A6
A1	1	0.906	0.571	0.690	0.341	0.356
A2	0.906	1	0.535	0.702	0.424	0.463
A3	0.571	0.535	1	0.547	0.289	0.428
A4	0.69	0.702	0.547	1	0.357	0.430
A5	0.341	0.424	0.289	0.357	1	0.746
A6	0.356	0.463	0.428	0.43	0.746	1

Table 2 shows the correlation coefficients between each module. The correlation coefficient ranges from 0 to 1, and the closer the value is to 1, the higher the degree of correlation between the two. The correlation coefficient between modules mostly ranges from 0.4 to 0.6. The correlation coefficient between A1 and A2 is 0.906, indicating a strong positive correlation, meaning that users have a high probability of watching the other module when watching either A1 or A2 module. In addition, the correlation coefficient between A5 and A6 modules is 0.746, indicating a strong positive correlation between the two. This indicates that there is a high correlation between modules A1 and A2, as well as A5 and A6. Drivers may also pay attention to module information with higher correlation while understanding the corresponding module information.

3.2 Optimization Analysis of HCI Based on SA-SSA Algorithm

Based on the above module coordinate system, the SA-SSA algorithm is used to obtain the optimal solution for the model. The parameter settings based on SA-SSA are as follows: population size of 100, safety factor of 0.6, initial and ending temperatures of 100 and 0.001, decay rate of 0.85, proportion of discoverers of 0.2, and proportion of warning persons of 0.1. Table 3 presents the optimal solutions based on each module.

In Table 3, Xup and Xdown represent the range of values for the upper and lower boundaries of the module based on the x-axis. Yup and Ydown are the values of the upper and lower boundaries of the model based on the Y-axis. The Xup and Xdown values of modules A1 and A2 exhibit an inverse relationship, meaning that the distribution of A1 and

A2 is axisymmetric with respect to the Y-axis. The field of view in this area is good, making it convenient for drivers to view the corresponding module data in real-time. Secondly, the positional information of A3 and A4 is distributed on both sides of the x-axis, exhibiting a mirror symmetric relationship with respect to the y-axis. The distribution of A5 and A6 does not show any symmetry, but they are located at the same horizontal level, which is convenient for drivers to observe. The HCI distribution of each module in autonomous vehicle obtained by SA-SSA algorithm is more reasonable. By placing modules with high relevance in visually closer proximity, the driver's line-of-sight movement and cognitive load can be reduced and interaction efficiency can be improved. By analyzing the data on the distribution of modules, researchers can better understand how much attention users pay to each module and the importance of these modules in user interface design. This information is important for optimizing the AR-HUD interface design and improving the interaction experience and safety of self-driving cars.

This study further examines the stability and computational efficiency of SA-SSA, as shown in Fig.9.

Table 3. Comparison of optimal solution of module coordinate information

Module coordinate information	Xup	Xdown	Yup	Ydown
A1	-40.11~40.11	-120.12~120.12	0	-240.12
A2	-120.12~120.12	-120.12~120.12	160.24	21.02
A3	160.22~423.12	160.22~423.12	-42.58	-122.25
A4	-423.12-160.22	-423.12-160.22	-42.58	-122.25
A5	-423.12-160.22	-423.12-160.22	200.36	240.12
A6	-112.56~438.58	-112.56~438.58	200.36	240.12

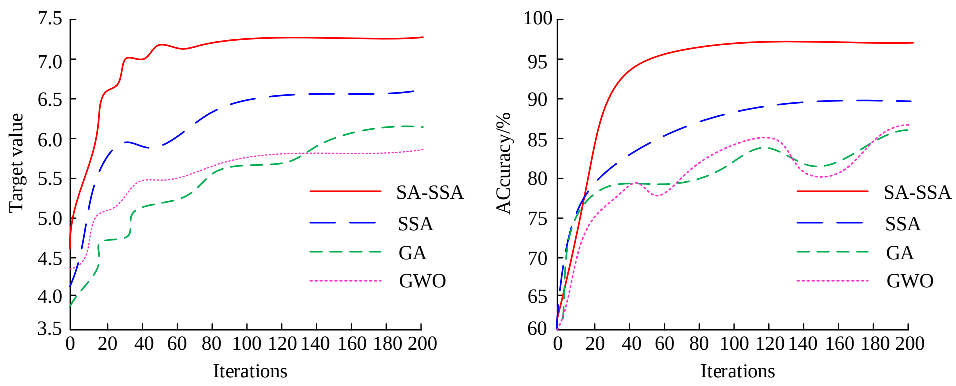

(a) Target value curve comparison
(b) Accuracy curve comparison

Figure 9: The target value of algorithm is compared with the accuracy curve

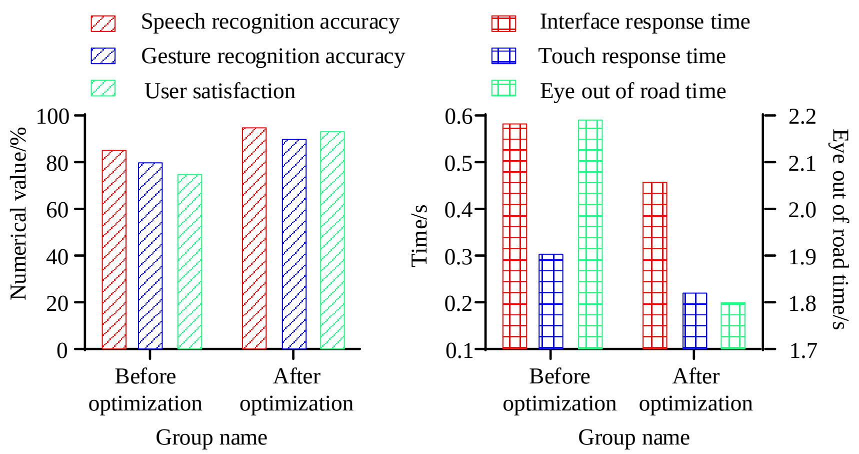

(a) Recognition accuracy is the comparison of user satisfaction
(b) Time comparison before and after optimization

Figure 10: Comparison of time and accuracy before and after optimization

Figs.9 (a) and (b) compare the target values and accuracy curves of four algorithms. In Fig.9 (a), the SA-SSA algorithm converges after 60 iterations, and the target value converges to around 7.22, which is higher than other algorithms. Due to the lack of SA algorithm optimization, the difference between SSA and SA-SSA in terms of target value convergence is relatively small. As GA and GWO iterate, there is a certain fluctuation in the target values, and their target values eventually converge to around 5.98 and 5.74. In Fig.9 (b), the accuracy of SA-SSA is significantly higher than other algorithms after convergence, with a value of 95.89%. Next is SSA, which converges at iteration 120 with an accuracy rate of around 88.36%. There is a certain degree of fluctuation in the accuracy curves of GA and GWO, with accuracies of 84.97% and 85.21% at iteration 200. In conclusion, SA-SSA algorithm has significant advantages in the process of solving the model, and the design scheme of HCI module of autonomous vehicle based on this algorithm is more excellent. Finally, this study selects 200 college students with over 1 year of driving experience and no color weakness to evaluate the interface parameters before and after optimization, as shown in Fig.10.

Fig.10 (a) shows the comparison of voice gesture accuracy and user satisfaction of autonomous vehicle before and after HCI optimization. The accuracy of optimized speech recognition technology has increased from 85.12% to 95.32%, it shows that the optimized interface is more accurate in speech recognition, and the user has a higher success rate of interacting with the system through voice commands. Gesture recognition technology has increased from 80.24% to 90.67%, it shows that the optimized interface also improves gesture recognition, and the accuracy of user control through gesture is increased. User satisfaction has increased from 70% to 85%. Fig.10 (b) shows the comparison of time before and after interface design optimization. The interface response, touch technology response, and line of sight departure time decrease from 0.581s to 0.462s, 0.302s to 0.212s, and 2.181s to 1.803s, respectively. It shows that the system responds to the user's operation faster, which can reduce the user's waiting time and improve the interaction efficiency. At the same time, users take their eyes off the road for less time while viewing interface information, thus reducing driving risks. In conclusion, after optimization, the recognition accuracy and response time of autonomous vehicle HCI have been optimized, which can provide more effective information and comfortable experience for drivers.

4. Discussion

This study improved the SA model by separating decision information and action sequence information from SA, reflecting the prerequisite of SA in drivers making decision information and taking corresponding measures. It obtains a set of icon samples by building a crawler program, and optimizes icon extraction through in-depth interviews. It uses entropy weight method to screen and evaluate icons. This process not only improves the quality and applicability of the icon sample set, but also characterizes the comprehensive score of the icon through the calculation of information entropy and weight values. By analyzing the visual area of the AR-HUD interface, it was found that there is a strong positive correlation between modules A1 and A2, A5 and A6. This indicates that when the driver payed attention to a module, he was likely to pay attention to the module with high correlation, which is of great significance for the information layout in the interface design. In algorithm optimization analysis, the SA-SSA algorithm outperformed the comparison algorithms in terms of iteration times and target values when seeking the optimal solution for the model. In the optimized interface parameter evaluation, the accuracy of speech recognition and gesture recognition technology increased from 85.12% to 95.32%, 80.24% to 90.67%, and user satisfaction increased from 70% to 85%. In addition, the interface response time, touch technology response time, and line of sight departure time have all been significantly reduced. Yamin P A R et al. improved automotive HCI based on AR-HUD. Similar to the research, this study designed 9 criteria that divided the area into vehicle status information, environmental information, and user information. These modules were also involved in the research. At the same time, this study discussed the possibility of machine learning algorithms optimizing HCI and demonstrated the effectiveness of using SA-SSA to optimize page layout [19]. Wu Z et al. evaluated the assisted-driving effects of different AR-HUD based on the SA model. This study indicated that in HCI, the importance of vehicle maintenance information was highest. This is consistent with the data results regarding A1 in this study. This study revealed that the importance of user information modules in HCI is relatively low, which is also addressed in the research results [20]. In conclusion, the AR-HUD design based on SA model can effectively improve the interactive experience and safety of autonomous vehicle. The application of SA-SSA algorithm further proves the effectiveness of the optimization scheme. In addition, considering that the driving scenarios of self-driving cars change dynamically, future research can explore the development of dynamic adaptive AR-HUD interfaces, which can automatically adjust the interface layout and information display according to the real-time road conditions and the driver's state (e.g., fatigue, concentration level), which will help to further reduce the cognitive load on the driver and improve driving safety. Meanwhile, HMI design for autonomous vehicles involves multiple disciplines such as psychology, cognitive science, computer science and traffic engineering, etc. Strengthening interdisciplinary cooperation and optimizing HMI design from a multidisciplinary perspective can provide more comprehensive support for the user experience and safety of autonomous vehicles.

5. Conclusions

This research deeply discussed the HCI design in autonomous vehicle, and proposed a new interface design scheme by optimizing the SA model and combining AR-HUD technology. Based on the SA-SSA algorithm, the HCI module was optimized and designed, and it was found that the optimized HCI page can provide more assistance for drivers' driving. Strong correlation between modules provides an important guideline for interface design. During the information layout, modules with high correlation should be placed in visually closer positions to reduce the driver's visual movement and cognitive load. Meanwhile the numerical results show that the optimized interface achieves significant improvement in both accuracy and response time. For example, the significant improvement in voice recognition accuracy means that the system is able to understand commands more accurately when the driver uses the voice interaction function, reducing the risk of misuse. The shortened response time of the interface shows that the system can respond to the driver's operation more quickly, reducing the waiting time for the driver and improving the efficiency of the interaction. Although this study has achieved certain results, there are still some limitations. The research sample may not be broad enough, as it mainly focuses on college students with certain driving experience, which may limit the generalizability of the research results. In addition, the complexity of the actual driving environment far exceeds laboratory conditions, so further adjustments and optimizations may be needed in practical applications. Future research can expand the data sample to include drivers of different ages, genders, and driving experiences, to improve the representativeness and applicability of research results. More advanced algorithms and AI technologies can also be introduced to further improve the performance and user experience of autonomous vehicle HCI.

Fundings

The research is supported by: General Project of Humanities and Social Sciences in Henan Province Universities, Research and Application of Factor Analysis Entropy Weight Method and Morphological Grammar for Extracting Cultural Factors from the Yellow River, (NO. 2024-ZZJH-352); Training Plan for Young Backbone Teachers in colleges and universities of Henan Province in 2024, Research on Design of age-appropriate service robots based on KANO and Morphological Grammar, (No. Education Office Gao (2024) 275).

References

[1] Tan, K., Wu, J., & Zhou, H. (2024). Integrating advanced computer vision and AI algorithms for autonomous driving systems. *Journal of Theory and Practice of Engineering Science,* 4(1), 41–48.

[2] Hasanvand, M., Nooshyar, M., & Moharamkhani, E. (2023). Machine learning methodology for identifying vehicles using image processing. *Artificial Intelligence and Applications,* 1(3), 170–178.

[3] Xia, T., Lin, X., & Sun, Y. (2023). An empirical study of the factors influencing users' intention to use automotive AR-HUD. *Sustainability,* 15(6), 5028–5039.

[4] You, F., Zhang, J., & Zhang, J. (2024). A novel cooperation-guided warning of invisible danger from AR-HUD to enhance driver's perception. *International Journal of Human–Computer Interaction,* 40(8), 1873–1891.

[5] Jiang, Q., & Guo, Z. (2023). AR-HUD optical system design and its multiple configurations analysis. *Photonics,* 10(9), 954–968.

[6] Fan, C., Kong, L., & Yang, B. (2023). Design of dual-focal-plane AR-HUD optical system based on a single picture generation unit and two freeform mirrors. *Photonics,* 10(11), 1192–1206.

[7] Goodge, T. A., Pollick, F., & Brewster, S. A. (2024). Can you hazard a guess? Evaluating the effect of augmented reality cues on driver hazard prediction. *Proceedings of the CHI Conference on Human Factors in Computing Systems,* 7(3), 1–28.

[8] Bing, W. (2023). Research on human-computer interaction system of intelligent connected vehicle based on computer AI artificial intelligence technology. *2023 IEEE International Conference on Image Processing and Computer Applications (ICIPCA),* 7(3), 603–608.

[9] Li, J., Jiang, F., & Yang, J. (2023). Lane-DeepLab: Lane semantic segmentation in automatic driving scenarios for high-definition maps. Neurocomputing, 465(2): 15-25.

[10] Tiwari, T., & Saraswat, M. (2023). A new modified-unet deep learning model for semantic segmentation. Multimedia Tools and Applications, 82(3): 3605-3625.

[11] Röckel, C., & Hecht, H. (2023). Regular looks out the window do not maintain situation awareness in highly automated driving. *Transportation Research Part F: Traffic Psychology and Behaviour,* 98(5), 368–381.

[12] Li, Y., Huang, Y., & Seneviratne, S. (2022). From traffic classes to content: A hierarchical approach for encrypted traffic classification. Computer Networks, 212(4): 109017-109033.

[13] Grivel, E., Berthelot, B., & Colin, G. (2024). Benefits of zero-phase or linear phase filters to design multiscale entropy: Theory and application. *Entropy,* 26(4), 332–350.

[14] He, J., Wang, G., & Yu, H. (2023). Generalized minimum error entropy Kalman filter for non-Gaussian noise. *ISA Transactions,* 136(6), 663–675.

[15] Rasappan, P., Premkumar, M., & Sinha, G. (2024). Transforming sentiment analysis for e-commerce product reviews: Hybrid deep learning model with an innovative term weighting and feature selection. *Information Processing & Management,* 61(3), 103654–103668.

[16] Kirsch, C., & Wendt, T. (2023). Computationally-efficient simulation of late reverberation for inhomogeneous boundary conditions and coupled rooms. *Journal of the Audio Engineering Society,* 71(4), 186–201.

[17] Li, M., Xu, J., & Wang, Z. (2024). Optimization of the Semi-Active-Suspension Control of BP Neural Network PID Based on the Sparrow Search Algorithm. Sensors, 24(6): 1757-1773.

[18] Xue, J., Shen, B., & Pan, A. (2023). An intensified sparrow search algorithm for solving optimization problems. *Journal of Ambient Intelligence and Humanized Computing,* 14(7), 9173–9189.

[19] Yamin, P. A. R., Park, J., & Kim, H. K. (2024). In-vehicle human–machine interface guidelines for augmented reality head-up displays: A review, guideline formulation, and future research directions. *Transportation Research Part F: Traffic Psychology and Behaviour,* 104(4), 266–285.

[20] Wu, Z., Zhao, L., & Liu, G. (2024). The effect of AR-HUD takeover assistance types on driver situation awareness in highly automated driving: A 360-degree panorama experiment. *International Journal of Human–Computer Interaction,* 40(20), 6492–6509